www.nature.com/aps

Acta Pharmacologica Sinica

ARTICLE

Ganoderic acid hinders renal fibrosis via suppressing the TGF-β/Smad and MAPK signaling pathways

Xiao-qiang Geng[1], Ang Ma[1], Jin-zhao He[1], Liang Wang[1], Ying-li Jia[1], Guang-ying Shao[1], Min Li[1], Hong Zhou[1], Shu-qian Lin[2,3], Jian-hua Ran[4] and Bao-xue Yang[1,5]

Renal fibrosis is considered as the pathway of almost all kinds of chronic kidney diseases (CKD) to the end stage of renal diseases (ESRD). Ganoderic acid (GA) is a group of lanostane triterpenes isolated from *Ganoderma lucidum*, which has shown a variety of pharmacological activities. In this study we investigated whether GA exerted antirenal fibrosis effect in a unilateral ureteral obstruction (UUO) mouse model. After UUO surgery, the mice were treated with GA (3.125, 12.5, and 50 mg· kg^{-1} ·d^{-1}, ip) for 7 or 14 days. Then the mice were sacrificed for collecting blood and kidneys. We showed that GA treatment dose-dependently attenuated UUO-induced tubular injury and renal fibrosis; GA (50 mg· kg^{-1} ·d^{-1}) significantly ameliorated renal disfunction during fibrosis progression. We further revealed that GA treatment inhibited the extracellular matrix (ECM) deposition in the kidney by suppressing the expression of fibronectin, mainly through hindering the over activation of TGF-β/Smad signaling. On the other hand, GA treatment significantly decreased the expression of mesenchymal cell markers alpha-smooth muscle actin (α-SMA) and vimentin, and upregulated E-cadherin expression in the kidney, suggesting the suppression of tubular epithelial-mesenchymal transition (EMT) partially via inhibiting both TGF-β/Smad and MAPK (ERK, JNK, p38) signaling pathways. The inhibitory effects of GA on TGF-β/Smad and MAPK signaling pathways were confirmed in TGF-β1-stimulated HK-2 cell model. GA-A, a GA monomer, was identified as a potent inhibitor on renal fibrosis in vitro. These data demonstrate that GA or GA-A might be developed as a potential therapeutic agent in the treatment of renal fibrosis.

Keywords: chronic kidney disease; renal fibrosis; ganoderic acid; epithelial-mesenchymal transition; TGF-β; UUO mice; HK-2 cells (human proximal tubular epithelial cells)

Acta Pharmacologica Sinica (2020) 41:670–677; https://doi.org/10.1038/s41401-019-0324-7

INTRODUCTION

Renal fibrosis is considered to be the pathway involved in almost all types of chronic kidney disease (CKD) [1–3]. The prevalence of CKD in the general population is high, reaching 13% in some countries and is increasingly becoming a public health problem worldwide [4–6]. For most CKD patients that reach end stage of renal disease (ESRD), dialysis and kidney transplantation are the only therapeutic options. The 5-year survival rate of people with ESRD on dialysis is 13%–60% lower than that of people of similar ages in the general population [7]. Importantly, only 25% of patients with ESRD undergo kidney transplantation in a timely manner, whereas 6% of patients die each year while waiting for a transplant [8]. In CKD, fibrosis is an active biosynthetic healing response initiated to protect tissue from injury. However, fibrosis can lead to serious organ damage when it becomes independent from the initial stimulus. However, approaches to attenuate or reverse renal fibrogenesis are limited [8, 9]. Recently, natural products have been studied in the search for novel and promising alternative drugs for preventing and treating fibrosis [10].

Ganoderma lucidum (*G. lucidum*), a well-known Chinese traditional medicine [11], has been used as a dietary supplement or drug to increase energy, improve immunity, and promote health and longevity for over 2000 years in Asian countries. Numerous bioactive constituents of *G. lucidum*, including terpenes, proteins, polysaccharides, amino acids, flavonoids, alkaloids, steroids, mannitol, and other compounds, have been revealed [12]. Pharmacological studies have determined that *G. lucidum* polysaccharides and triterpenes have multiple pharmacological activities [13–16].

We recently studied the therapeutic effect of Ganoderma triterpenoids (GTs) on autosomal dominant polycystic kidney disease (ADPKD) [15] and hyperhomocysteinemia (HHcy)-induced endothelial injury [14]. GTs exerts a fascinating inhibitory effect on renal cyst development in an ADPKD mouse model via down-regulating Ras/mitogen-activated protein kinase (MAPK) signaling and promoting cell differentiation [15]. It was determined that, in a bovine aortic endothelial cell model, GT protects against HHcy-induced EMT via inhibiting canonical TGF-β/Smad- and non-Smad-dependent signaling pathways [14]. Considering the common

[1]State Key Laboratory of Natural and Biomimetic Drugs, Department of Pharmacology, School of Basic Medical Sciences, Peking University, Beijing 100191, China; [2]Fuzhou Institute of Green Valley Bio-Pharm Technology, Fuzhou 350002, China; [3]JUNCAO Technology Research Institute, Fujian Agriculture and Forestry University, Fuzhou 350002, China; [4]Department of Anatomy, and Laboratory of Neuroscience and Tissue Engineering, Basic Medical College, Chongqing Medical University, Chongqing 400016, China and [5]Key Laboratory of Molecular Cardiovascular Sciences, Ministry of Education, Beijing 100191, China
Correspondence: Bao-xue Yang (baoxue@bjmu.edu.cn)

Received: 7 July 2019 Accepted: 20 September 2019
Published online: 5 December 2019

pathogenesis and signaling pathways, these data strongly suggest that GTs and their components can be developed as novel agents for preventing and treating CKD.

Ganoderic acid (GA), as one of the most abundant GTs, has been reported to have multiple therapeutic activities, such as antibacterial, antiviral, antitumor, hepatoprotective, antioxidative, antihypertensive, and antiaggregation activities [11]. GA-A, GA-B, and GA-C2 are representative active components and the most abundant components of crude GA. In addition, GA-A is viewed as a marker for evaluating *G. lucidum* quality [17] and has been reported to exhibit antioxidative, cytotoxic, hepatoprotective, and anticancer activities [18–20].

In this study, we used a unilateral ureteral obstruction (UUO) mouse model to identify the antirenal fibrotic effect of GA. A TGF-β1-stimulated HK-2 cell model was used to identify the antifibrotic effects of active compounds of GA and reveal the related mechanisms. The experimental results showed that GA significantly inhibited the progression of renal fibrosis partially via suppressing the TGF-β/Smad and MAPK signaling pathways. The monomer GA-A, which was isolated from GA, had a potent antirenal fibrotic effect.

MATERIALS AND METHODS

Ganoderic acid preparation

The purified natural product GA and three monomers (GA-A, B, and C2) were extracted and isolated from *G. lucidum*. In the in vivo experiment, GA was dissolved in saline with 5% Tween 80. GA and these three monomers were dissolved in DMSO for the in vitro experiment. According to the results of HPLC, the concentrations of GA-A, GA-B, and GA-C2 were 16.101, 10.586, and 5.404 μg/mL, respectively. These three monomers accounted for 16.1% (GA-A), 10.6% (GA-B), and 5.4% (GA-C2) of crude GA. The purity of these three monomers was >98%, as determined by HPLC [21].

Cell culture

The HK-2 cells (human proximal tubular epithelial cells) were gifted by Dr Hui-wen Ren at Tianjin Medical University, Tianjin, China. Briefly, the HK-2 cells were cultured in DMEM/F12 containing 8% fetal bovine serum (FBS; Gibco, Australia), 2 mM glutamine, 100 U/mL penicillin, and 100 μg/mL streptomycin in a humidified atmosphere with 5% CO_2 at 37 °C. When the cells reached 40%–50% confluence, they were incubated with 10 ng/mL TGF-β1 with or without test compounds, all of which were dissolved in DMSO (0.1%), for 48 h. To identify the underlying mechanisms, the cells were incubated with 10 ng/mL TGF-β1 with or without test compounds dissolved in DMSO (0.1%) for 1 h. Specifically, DMSO was adopted as the solvent for the control group.

Cytotoxicity assay

The CCK-8 assay kit (Dojindo, Kumamoto, Kyushu, Japan) was used to test cytotoxicity in vitro. HK-2 cells were plated in 96-well plates at a density of 5000 cells/well. HK-2 cells were incubated with GA (mix, A, B, and C2) for 24 h. Then, the CCK-8 solution diluted 1/10 with 8% FBS DMEM/F12, was added to each well, and the cells were incubated for 2 h at 37 °C. The absorbance at 450 nm was measured with a microplate reader (Biotek, MQX200, Winooski, VT, USA). Cell viability was calculated as follows:

$$\text{Cell viability}\ (\%) = (OD_{\text{treatment}} - OD_{\text{blank}}) / (OD_{\text{control}} - OD_{\text{blank}}) \times 100$$

Mouse UUO model

The UUO model was established in male C57BL/6J mice (8 weeks of age, 25–30 g body weight, purchased from the Animal Center of Peking University Health Science Center, Beijing, China), which were housed with a 12-h/12-h light/dark cycle with food and water available ad libitum. The mice were randomly divided into experimental groups, including the sham plus vehicle control (5% Tween 80 dissolved in saline) group, the sham plus 50 mg/kg GA group, the UUO plus vehicle control group, and the UUO plus 3.125, 12.5, and 50 mg·kg^{-1}·day^{-1} GA groups. UUO was performed as follows: the abdominal cavity was exposed by a midline incision, and the left ureter was isolated and ligated. The sham group only received incision as a control [22, 23].

To examine the efficacy of GA in renal fibrosis after UUO injury, GA was intraperitoneally administered at a concentration of 3.125, 12.5, or 50 mg·kg^{-1}·day^{-1} for 7 or 14 days beginning immediately after UUO. Seven or 14 days after surgery, the animals were sacrificed, and the blood and kidneys were collected for biochemical and protein analysis and histologic examination.

BUN and blood creatinine measurement

The urea concentration in the blood was measured using a QuantiChrom Urea Assay kit (BioAssay Systems, Hayward, CA, USA). The creatinine concentration in the blood was measured with commercial kits (NJJC Bio, Nanjing, Jiangsu, China) according to the manufacturer's instructions.

Renal histologic staining and ultrastructural examination

Kidneys were collected and fixed in 4% paraformaldehyde in 0.01 M phosphate-buffered saline (PBS) overnight, dehydrated, embedded in paraffin, and cut into 5-μm sections. After deparaffinization, the kidney tissue sections were rehydrated and stained with hematoxylin and eosin and Masson's trichrome. Tissue damage was assessed based on the tubular damage score, as previously described [24]. Briefly, injury was scored in a blinded manner according to the percentage of damage, which included the loss of the brush border, tubular dilation and intertubular hemorrhage (0 = normal; 1 ≤ 20%; 2 = 20%–40%; 3 = 40%–60%; 4 = 60%–80%; and 5 ≥ 80%). Representative fields were captured.

For ultrastructural evaluation, kidneys that were cut into 1 mm^3 pieces were fixed in 2.5% glutaraldehyde, postfixed in osmium tetroxide, and stained with uranyl acetate and lead citrate. The specimens were thinly sectioned and examined under a transmission electron microscope. Electron microscopy images were randomly taken for each group.

Western blot analysis

Renal tissues or cells were homogenized in tissue protein extraction reagent (Mei5, MF188-01, Beijing, China) containing a protease inhibitor cocktail (Roche, Basel, Kanton Basel-Stadt, Switzerland). Total protein was measured by the BCA method (Pierce, Rockford, IL, USA). The lysates were electrophoresed on polyacrylamide gels and electrotransferred to polyvinylidene difluoride membranes (Amersham Biosciences, Boston, MA, USA). After blocking, the membranes were incubated with antibodies against GAPDH (Proteintech, 60004-1-lg, 1:5000 dilution, Rosemont, PA, USA), fibronectin (Proteintech, 15613-1-AP, 1:1000 dilution), α-SMA (ACTA2, ABclonal, A1011, 1:1000 dilution, Wuhan, Hubei, China), TGF-β (CST, 3711, 1:1000 dilution, Danvers, MA, USA), Smad2 (CST, 5339, 1:1000 dilution), p-Smad2/3 (abcam, ab63399, 1:1000 dilution, San Francisco, CA, USA), Smad7 (ABclonal, A12343, 1:1000 dilution), E-cadherin (CST, 24E10, 1:1000 dilution), vimentin (CST, 5741, 1:1000 dilution), CTNNB1 (β-catenin, ABclonal, A11512, 1:1000 dilution), p-JNK (CST, 9255, 1:1000 dilution), JNK (ABclonal, A1251, 1:1000 dilution), p-ERK (CST, 4370, 1:2000 dilution), ERK2 (ABclonal, A11186, 1:1000 dilution), p-p38 (CST, 4511, 1:1000 dilution), and p38 (CST, 8690, 1:1000 dilution). Goat anti-rabbit IgG or goat anti-mouse IgG (EASYBIO, Beijing, China) was added, and the blots were developed with an ECL plus kit (Biodragon, Beijing, China) and visualized with a chemiluminescence detection system (Syngene, GeneGnome XRQ, Cambridge, Cambridgeshire, UK). Quantitation was performed by scanning and analyzing the intensity of the hybridization bands.

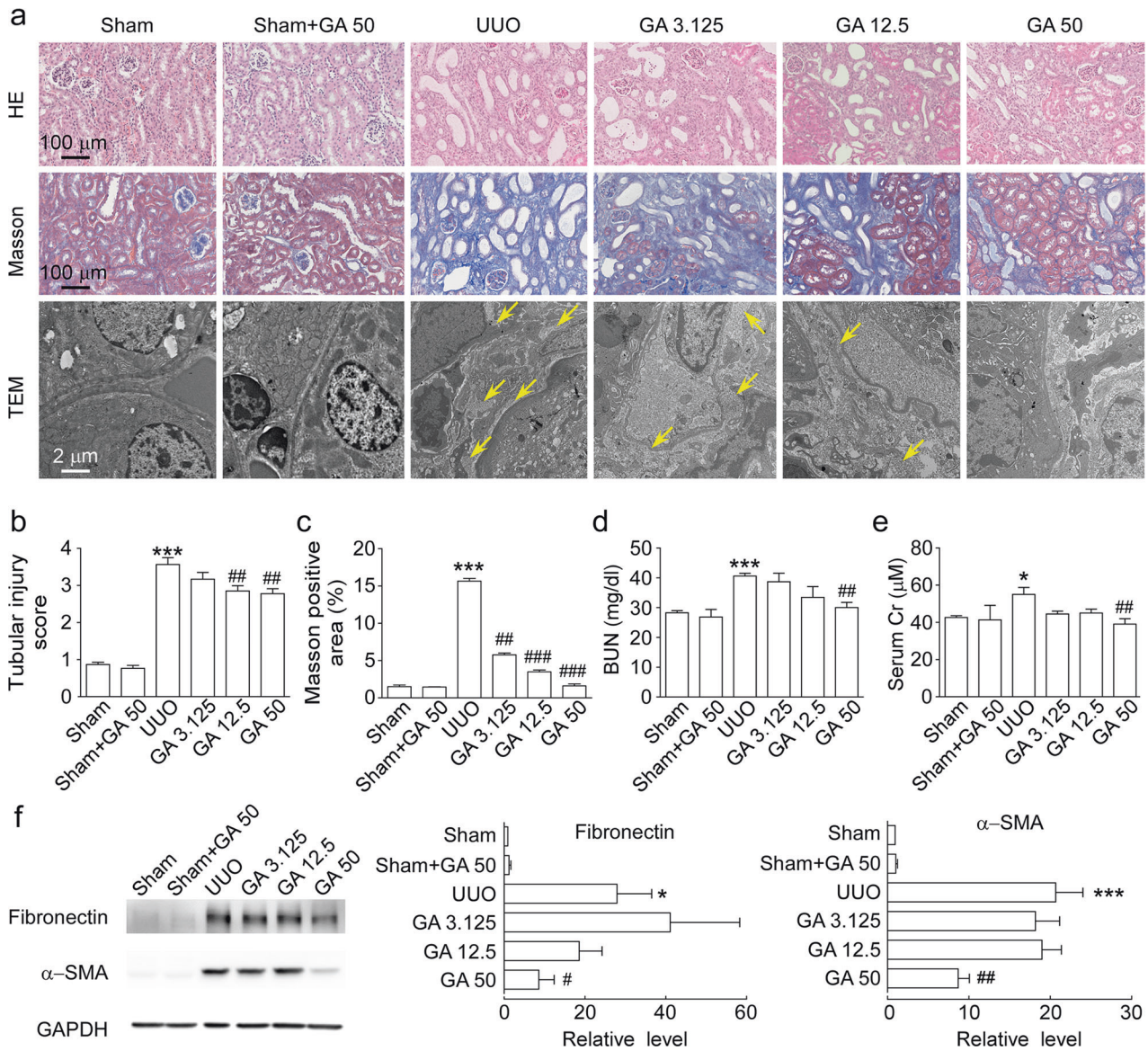

Fig. 1 GA hindered tubular injury and renal fibrosis induced by UUO. GA at a concentration of 3.125, 12.5, or 50 mg/kg or vehicle control was intraperitoneally administered to C57BL/6J male mice for 14 days beginning immediately after UUO surgery. **a** Representative micrographs of H&E staining (magnification of ×200, top panel), Masson's trichrome staining (magnification of ×200, middle panel, typical renal fibrosis is represented by collagen deposition stained blue) and transmission electron microscopy (TEM) (magnification of ×6000, bottom panel, typical interstitial fibers are indicated by yellow arrows). **b** Quantification of tubular injury scores. **c** Masson-positive area quantified using ImageJ software. **d** BUN level. **e** Serum creatinine level. **f** Representative Western blot for fibronectin and α-SMA (left) and the relative protein levels of fibronectin and α-SMA in the kidneys (middle and right). The data were normalized to the intensity of GAPDH and are expressed relative to the value of the Sham group. The data are presented as the mean ± SEM ($n = 6$). $^{*}P < 0.05$, $^{***}P < 0.001$ versus the Sham group; $^{\#}P < 0.05$, $^{\#\#}P < 0.01$, $^{\#\#\#}P < 0.001$ versus the UUO group.

Immunohistochemical staining and laser confocal microscopy

The expression of the epithelial-to-mesenchymal transition (EMT) marker α-SMA in the kidneys was evaluated by immunohistochemistry and laser confocal microscopy. Briefly, the kidneys were fixed with 4% paraformaldehyde in PBS for 24 h and incubated with 30% sucrose overnight at 4 °C. The sections were embedded in optimal cutting temperature medium and cut into 5-μm-thick tissue sections. The sections were dewaxed and hydrated in graded ethanol solutions and then microwaved in sodium citrate buffer. The endogenous peroxidase activity was blocked using 3% H_2O_2 for 10 min at room temperature. The samples were blocked with 5% goat serum for 30 min and then treated with a primary antibody against α-SMA (1:200) at 4 °C overnight. The next day, the sections were incubated with the goat anti-rabbit IgG secondary antibody for 30 min at 37 °C. Then, the sections were stained with 3,3'-diaminobenzidine and counterstained with hematoxylin. After dehydrating and drying, the sections were mounted with neutral gum and observed under a microscope. Laser confocal microscopy was performed as previously described [25, 26].

Statistical analysis

Statistical analyses were performed using GraphPad Prism software (San Diego, CA, USA). All results are expressed as the means ± SEM. Each experiment was performed at least three times. A two-tailed *t* test, one-way ANOVA analysis of variance followed by post hoc Bonferroni test, or a general linear model with repeated

measures followed by post hoc Bonferroni test was then performed to assess the differences between the groups. *P* values <0.05 were considered statistically significant.

RESULTS

GA hindered tubular injury and renal fibrosis induced by UUO

Based on research by Pillai et al., who found that treatment with 50 mg/kg *G. lucidum* terpenes exerts a renoprotective effect against cisplatin-induced nephrotoxicity [27], we chose 3.125–50 mg/kg GA for use in our in vivo study. GA was administered at concentrations of 3.125, 12.5, or 50 mg/kg via intraperitoneal injection once a day for 14 days beginning immediately after UUO surgery. Treatment with GA significantly reduced the tubular injury score (Fig. 1a, b), Masson-positive area (Fig. 1a, c) and fiber accumulation (Fig. 1a) in a dose-dependent manner. Compared with the low and medium doses, the high dose of GA (50 mg/kg) significantly lowered the BUN and blood creatinine concentrations (Fig. 1d, e) and thus ameliorated renal dysfunction during fibrotic progression. Moreover, the high dose of GA significantly decreased the expression of fibronectin and α-smooth muscle actin (α-SMA) in kidney tissue (Fig. 1f). These results indicate that GA exhibits potent antirenal fibrotic bioactivity at high doses. Therefore, 50 mg/kg GA was used for the subsequent experiments to explore the underlying mechanisms.

GA hindered renal tubular EMT progression in the UUO model

As expected, UUO mice developed typical renal EMT characterized by elevated expression of the mesenchymal cell marker α-SMA and vimentin and decreased expression of the epithelial cell marker E-cadherin compared with that in sham mice (Fig. 2a). Interestingly, Western blotting showed that GA markedly reversed the elevation of α-SMA and vimentin levels and the reduction in E-cadherin protein levels (Fig. 2a). Furthermore, laser confocal microscopy and immunohistochemical staining for α-SMA verified that GA downregulated the α-SMA protein levels in UUO mice (Fig. 2b). These results demonstrate that GA inhibits renal EMT in fibrotic kidneys.

GA downregulated the TGF-β/Smad and MAPK signaling pathways in vivo

To further explore the underlying mechanism, we examined whether GA affects the TGF-β-induced activation of Smad and non-Smad pathways in UUO mice. The protein levels of TGF-β, fibronectin, phosphorylated Smad2/3 and total Smad (represented by Smad2) were notably increased in UUO mice compared with sham group mice (Fig. 3a, c). GA significantly attenuated TGF-β expression, TGF-β-induced Smad2/3 phosphorylation, and total Smad levels. As the inhibitory component, Smad7 is able to inhibit renal fibrosis in a number of experimental models of CKD mainly by blocking Smad2/3 activation and anti-inflammation [28]. We found obviously decreased expression of Smad7 in fibrotic kidneys, which was significantly rescued by GA (Fig. 3a, c).

In addition to the TGF-β/Smad pathway, non-Smad signaling pathways, such as the MAPK signaling pathway, have been demonstrated to play a major role in EMT progression and in many pathophysiological processes associated with renal fibrosis [29–31]. Therefore, we used Western blotting to detect the activation of the MAPK signaling pathway in kidney tissue. The results showed that the phosphorylation levels of three key MAPK signaling proteins (ERK, JNK, and p38) were significantly increased in obstructed kidneys. GA significantly suppressed the phosphorylation of these proteins (Fig. 3b, c). Moreover, a previous study suggested that β-catenin levels are elevated in the UUO model and that Wnt/β-catenin signaling activation contributes to EMT in UUO nephropathy [32]. Many studies have also identified a link between β-catenin and EMT in many other diseases [33, 34]. Our results showed a remarkable reduction in β-catenin after 14 days of GA treatment in UUO mice (Fig. 3a, c). In addition, GA inhibited the activation of p38 (Fig. 3b, c). Taken together, these data suggest that GA potently partially downregulates both Smad and non-Smad signaling, thereby hindering renal fibrotic progression.

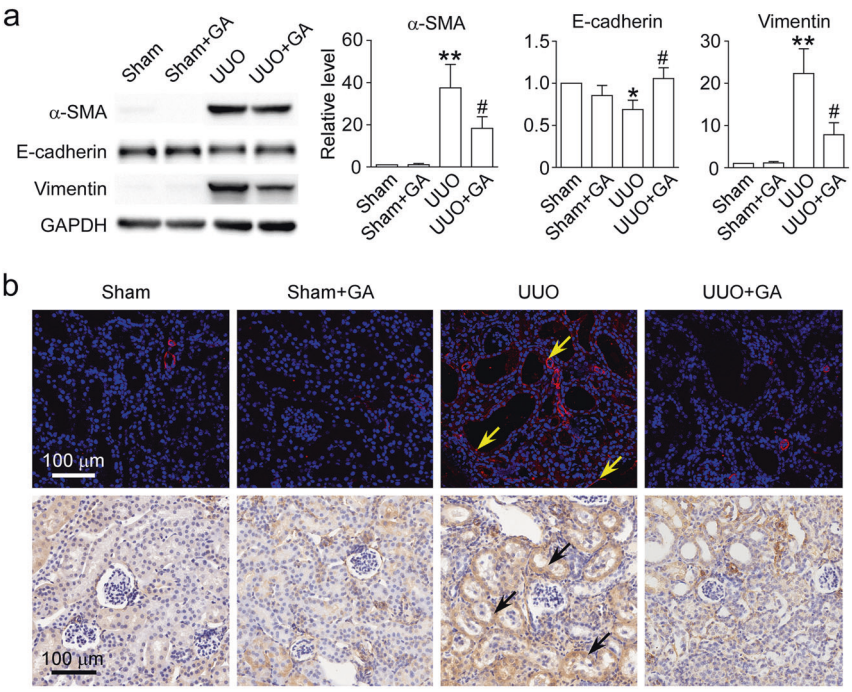

Fig. 2 GA hindered renal tubular EMT progression in the UUO mouse model. a Representative Western blot (left) and the relative protein levels of α-SMA, E-cadherin, and vimentin in the kidneys (right panel). The data were normalized to the intensity of GAPDH and are expressed relative to the value of the Sham group. **b** Representative micrographs of immunofluorescence (top panel) and immunohistochemical staining (bottom panel) with an α-SMA antibody (typical α-SMA positive cells are indicated by yellow or black arrows, magnification of ×200). The data are presented as the mean ± SEM ($n = 6–8$). $^{*}P < 0.05$, $^{**}P < 0.01$, versus the Sham group; $^{\#}P < 0.05$ versus the UUO group.

GA downregulated the TGF-β/Smad and MAPK signaling pathways in HK-2 cells

To confirm the suggested mechanisms, a TGF-β1-stimulated HK-2 cell model was adopted. As shown, the addition of TGF-β1 for 1 h significantly increased the phosphorylation levels of Smad2/3 and ERK/JNK/p38 in HK-2 cells (Fig. 4). According to our previous research experience, the terpenes isolated from *Ganoderma* exert their pharmacological activities often at doses between 6.25 and 100 μg/mL in vitro [14, 15, 35, 36]. Therefore, we chose 6.25, 25, and 100 μg/mL GA for the in vitro study. GA treatment obviously reduced the expression levels of phosphorylated Smad2/3 and phosphorylated ERK/JNK/p38 in a dose-dependent manner (Fig. 4). These data suggest that GA exerts its antirenal fibrotic activity partially by downregulating the TGF-β/Smad and MAPK signaling pathways both in vitro and in vivo.

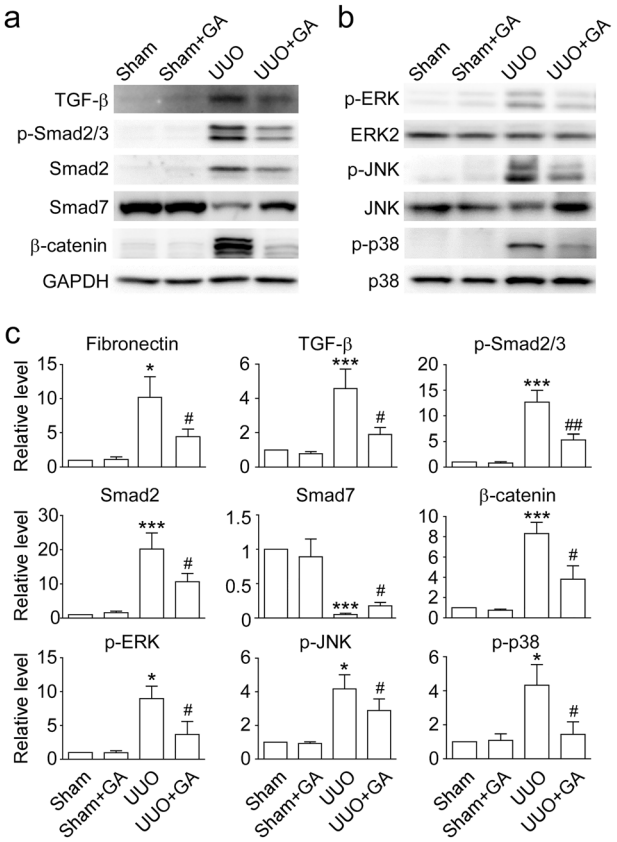

Fig. 3 GA inhibited the TGF-β/Smad and MAPK signaling pathways in vivo. Kidney proteins were extracted and used for Western blot analysis. **a** Representative Western blot for key proteins of the TGF-β/Smad signaling pathways. **b** Representative Western blot for key proteins of the TGF-β/non-Smad signaling pathways. **c** The relative protein levels in the experiments shown in **a** and **b**. The data were normalized to the intensity of GAPDH or the nonphosphorylated form and are expressed relative to the value of the Sham group. The data are presented as the mean ± SEM ($n = 6–8$). $^{*}P < 0.05$, $^{***}P < 0.001$ versus the Sham group; $^{\#}P < 0.05$, $^{\#\#}P < 0.01$ versus the UUO group.

The GA monomer GA-A was shown to be a potent inhibitor of renal fibrosis

To determine the compound with the strongest antifibrotic bioactivity, the monomers GA-A, GA-B, and GA-C2 were isolated and identified by HPLC (Fig. 5a); the concentrations of GA-A, GA-B, GA-C2 were 161.013, 105.864, and 54.041 μg/mL, respectively. A CCK-8 assay for cell viability revealed that GA mix, GA-A, GA-B, and GA-C2 at doses under 200 μg/mL had no cytotoxic effect on HK-2 cells (data not shown).

Cell morphology showed that HK-2 cells lost their epithelial appearance and presented elongated and spindle-shaped morphology after being stimulated with 10 ng/mL TGF-β1 for 48 h (Fig. 5b). GA-A (100 μg/mL) significantly reduced spindle-like morphology induced by TGF-β1 stimulation and decreased the expression of fibronectin. However, GA-B and GA-C2 at equivalent doses did not affect the morphological changes or the expression of fibronectin (Fig. 5b, c). It was also found that GA-A dose-dependently reversed the levels of fibrotic markers upregulated by TGF-β1 (Fig. 5d). These results indicate that GA-A potently inhibits renal fibrosis.

DISCUSSION

The UUO mouse model is widely accepted and has been widely adopted to investigate renal fibrotic mechanisms and to develop therapeutic strategies [22]. Ureteral obstruction results in marked renal dysfunction and morphological changes with excess deposition of ECM and renal fibrosis. Various researchers have used various obstruction durations (from 7 to 14 days) in the UUO mouse model [37, 38]. We found that, both 7 (data not shown) and 14 days after ureteral ligation, the obstructed kidneys showed typical features of tubular injury and interstitial fibrosis. Renal dysfunction, characterized by elevated BUN and serum creatinine levels, was more significant in the 14-day UUO model than in the 7-day UUO model. Consistently, the morphological changes, including tubular injury and ECM deposition, were more severe in the 14-day UUO kidneys. Western blot analysis also showed that fibronectin, collagen IV and α-SMA expression was increased more

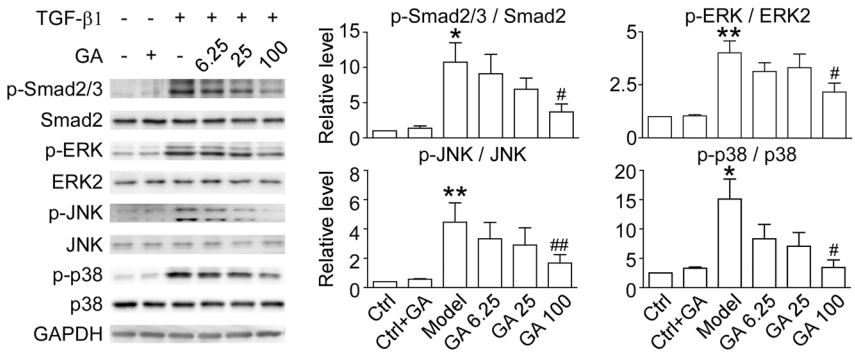

Fig. 4 GA inhibited the TGF-β/Smad and MAPK signaling pathways in HK-2 cells. Representative Western blot for key proteins of the TGF-β/Smad and MAPK signaling pathways (left) and the relative levels of phosphorylated and total proteins (right panel). The data were normalized to the intensity of total protein and are expressed relative to the value of the control (Ctrl) group. The data are presented as the mean ± SEM ($n = 4–6$). $^{*}P < 0.05$, $^{**}P < 0.01$ versus the Ctrl group; $^{\#}P < 0.05$, $^{\#\#}P < 0.01$ versus the Model group.

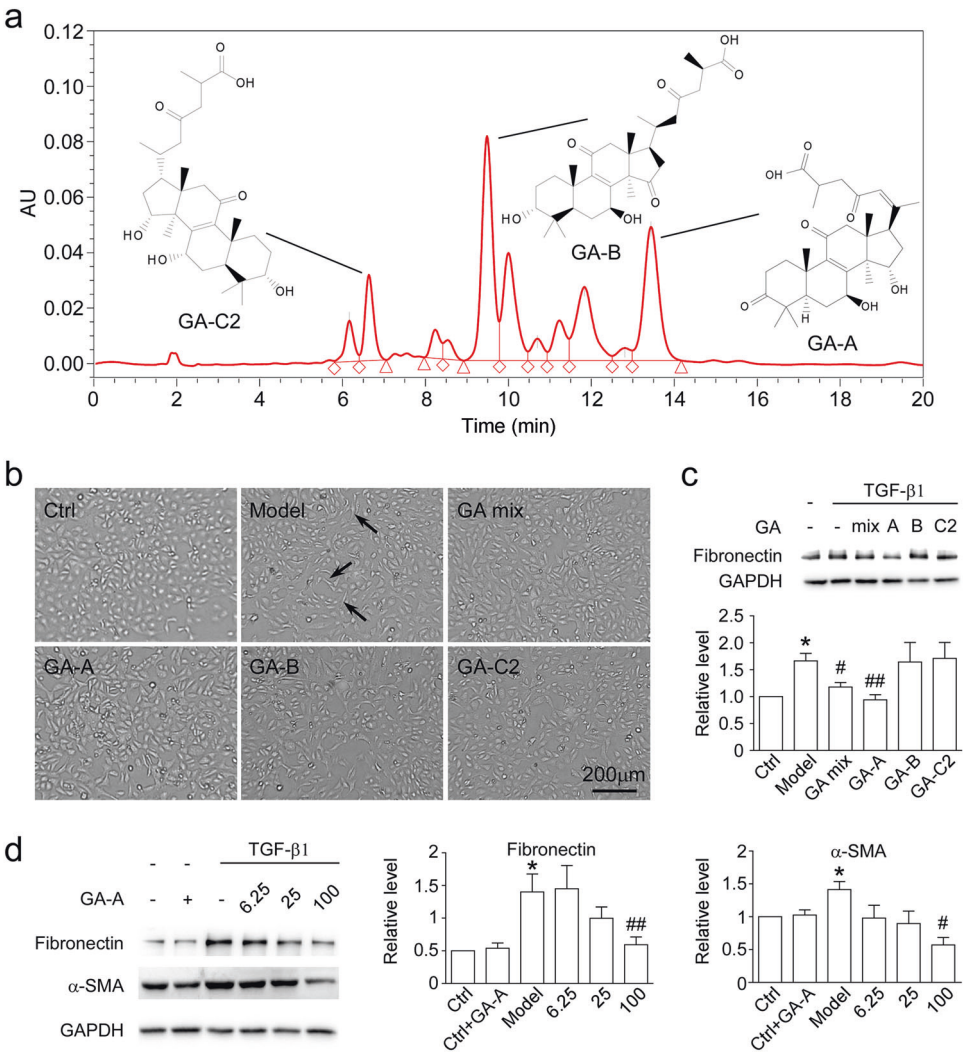

Fig. 5 Inhibitory effect of the GA monomers GA-A, GA-B, and GA-C on fibrosis in vitro. a The identification of GA-A, GA-B, and GA-C by HPLC. **b** Microscopy images showing morphological changes of HK-2 cells treated with or without TGF-β1, TGF-β1 and GA mix, TGF-β1 and GA-A, TGF-β1 and GA-B, and TGF-β1 and GA-C for 48 h. Elongated and spindle-like cells are indicated by arrows. **c** Fibronectin protein levels, as detected by Western blot analysis. **d** Fibronectin and α-SMA protein levels in the control group and groups treated with TGF-β1 and TGF-β1 plus GA-A at different concentrations, as detected by Western blot analysis (left). The data were normalized to the intensity of GAPDH and are expressed relative to the value of the control (Ctrl) (right panel). The data are presented as the mean ± SEM ($n = 4–6$). $^{*}P < 0.05$ versus the Ctrl group; $^{\#}P < 0.05$, $^{\#\#}P < 0.01$ versus the Model group.

obviously in the 14-day UUO kidneys. Therefore, we adopted the 14-day UUO model to determine the therapeutic effect of GA.

Using the UUO mouse model, we first demonstrated that GA significantly hindered renal fibrosis. GA inhibited morphologic changes and the expression of profibrotic and ECM proteins in a dose-dependent manner. In vivo, GA reduced the renal expression of fibronectin and collagen, and this effect was accompanied by the inhibition of EMT progression via decreasing α-SMA, vimentin levels and increasing E-cadherin levels, which indicates that GA prevented renal fibrosis mainly by inhibiting Smad and non-Smad signaling. Specifically, GA suppressed Smad2/3 phosphorylation and increased the expression of Smad7 in fibrotic kidneys, directly affecting the production and accumulation of ECM.

Renal tubular EMT is an important mechanism in the development of renal fibrosis [39–41]. Epithelial cells, through EMT, which is characterized by the reduced or absent expression of the epithelial intercellular adhesion E-cadherin and the increased expression of α-SMA, translocate from the epithelial compartment to the interstitium and gain a full mesenchymal phenotype, through which fibrotic matrix proteins, such as fibronectin and collagens, are produced [39, 42]. Many lines of research have demonstrated that the deletion of major transcriptional regulators of EMT, such as Twist and Snail, rescue renal fibrosis [43]. Therefore, developing a novel approach that inhibits EMT progression and ECM deposition would be an effective therapeutic option for inhibiting renal fibrosis and preserving renal function in CKD.

In renal fibrosis, TGF-β1 is considered a master regulator of EMT and ECM accumulation and consequently a potential key driver of renal fibrosis [44, 45]. TGF-β signals are transduced mainly by TGF-β receptor (TβR)-mediated Smad and non-Smad signaling. Upon TGF-β stimulation, regulatory Smads (Smad2 and Smad3, R-Smads) are recruited to TβRs and activated by phosphorylation. Subsequently, activated R-Smads heteroligomerize with Smad4 and translocate to the nucleus, where they jointly transactivate downstream profibrogenic protein expression [46], which can be inhibited by Smad7 [28] (Fig. 6). In the present study, the overexpression of TGF-β1 significantly induced the phosphorylation of Smad2/3, which directly activated the accumulation of fibronectin and collagen and EMT progression (Fig. 6).

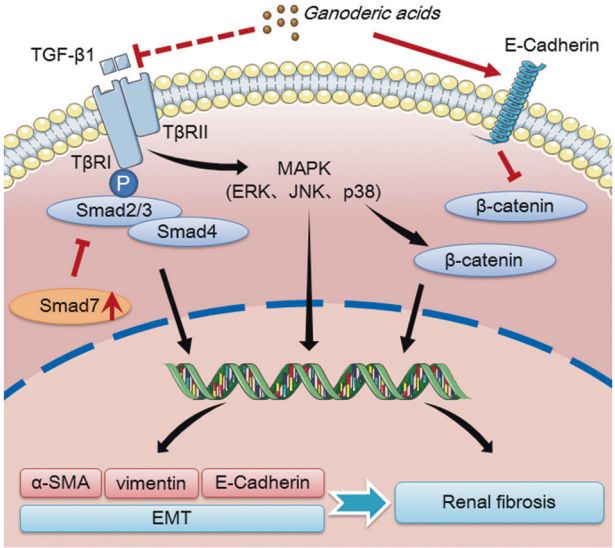

Fig. 6 Schematic diagram of the proposed underlying mechanisms involved in the antirenal fibrotic activity of GA. Please see the text for explanations.

It has been suggested that, as additional downstream pathways of TGF-β, the MAPK (ERK, JNK, and p38) signaling pathways are overactivated and promote the EMT process in obstructed kidneys and in TGF-β1-treated renal tubular epithelial cells [30, 47]. In 2008, it was reported that p38 MAPK leads to the accumulation of β-catenin via GSK3β signaling [48], which has been indicated to play an essential role in renal tubular EMT [42]. In addition, many studies have demonstrated that the MAPK pathways, as non-Smad signaling pathways, regulate EMT. The suppression of MAPK signaling pathways reverses EMT progression and renal fibrosis [30, 49–52]. Our present data showed that GA obviously partially downregulated the phosphorylation of ERK, JNK, and p38, indicating that the downregulation of the Smad-independent pathway also ameliorated renal fibrosis.

Above all, GA exhibited potent inhibitory bioactivity against TGF-β signaling in a mouse renal fibrosis model and in an HK-2 cell model via inhibiting the same signaling pathways. Considering that the TGF-β signaling pathway is closely associated with a number of fibrotic diseases, including renal fibrosis, lung fibrosis, hepatic fibrosis, atrial fibrosis, and cardiac fibrosis as well as the progression and metastasis of various cancers, connective tissue and skeletal diseases [53–55], GA might be developed as a potent drug to treat TGF-β signaling-related diseases more extensively.

GA-A, one of the representative active components and the most abundant component of crude GA, has been reported to exhibit various pharmacological activities. Jiang et al. reported that GA-A inhibits the growth and invasive behaviors of human breast cancer cells by modulating AP-1 and NF-κB signaling [18]. Radwan et al. proved that GA-A has anti-B-cell lymphoma potential, mainly through inducing apoptosis and mediating immune responses [56]. Das et al. found that GA-A plays a potent antitumorigenic role in meningioma by suppressing the Wnt/β-catenin signaling pathway [57].

We subsequently elucidated that GA-A is the most effective antirenal fibrotic component of GA. Because of the limited production of GA-A/B/C2, we only identified the effective monomer of GA through in vitro research. Further in vivo studies are necessary to investigate the relevance of our in vitro data using the UUO model. In our study, the treatment of fibrotic kidneys with GA significantly downregulated various downstream signals of TGF-β, suggesting that GA may target novel factors of renal fibrosis. However, the specific target of GA is another key question and should be further studied.

In conclusion, our study identified that GA possesses renoprotective activity, especially in hindering renal fibrosis, in a UUO mouse model. Based on our experimental data, we suggest a mechanism by which GA protects renal fibrosis. On the one hand, GA hinders the EMT process, partially by downregulating TGF-β signaling via downstream Smad and non-Smad pathways. In addition, GA also directly suppresses the deposition of ECM proteins, such as fibronectin, by inhibiting the activation of TGF-β/Smad2/3 signaling. Specifically, GA-A was identified as the monomer with the strongest protective effect against TGF-β1-stimulated fibrosis in HK-2 cells. Therefore, our study suggests that GA can be developed as a promising therapeutic agent to suppress the progression of renal fibrosis, providing a potential effective treatment for CKD.

ACKNOWLEDGEMENTS

This work was supported by the National Natural Science Foundation of China (grants 81620108029, 81330074, 81261160507, 81974083, 81170632 and 81770738) and the Beijing Natural Science Foundation (grant 7172113).

AUTHOR CONTRIBUTIONS

XQG and BXY designed the research. XQG, AM, JZH, YLJ, LW, GYS, ML, and JHR performed the research. XQG, JHR, and SQL analyzed the data. XQG and BXY wrote the manuscript. HZ and BXY revised the manuscript.

ADDITIONAL INFORMATION

Competing interests: The authors declare no competing interests.

REFERENCES

1. Zeisberg M, Neilson EG. Mechanisms of tubulointerstitial fibrosis. J Am Soc Nephrol. 2010;21:1819–34.
2. Boor P, Ostendorf T, Floege J. Renal fibrosis: novel insights into mechanisms and therapeutic targets. Nat Rev Nephrol. 2010;6:643–56.
3. Farris AB, Colvin RB. Renal interstitial fibrosis: mechanisms and evaluation. Curr Opin Nephrol Hypertens. 2012;21:289–300.
4. De Nicola L, Minutolo R. Worldwide growing epidemic of CKD: fact or fiction? Kidney Int. 2016;90:482–4.
5. Levin A, Tonelli M, Bonventre J, Coresh J, Donner JA, Fogo AB, et al. Global kidney health 2017 and beyond: a roadmap for closing gaps in care, research, and policy. Lancet. 2017;390:1888–917.
6. Zhang L, Wang F, Wang L, Wang W, Liu B, Liu J, et al. Prevalence of chronic kidney disease in China: a cross-sectional survey. Lancet. 2012;379:815–22.
7. Nordio M, Limido A, Maggiore U, Nichelatti M, Postorino M, Quintaliani G, et al. Survival in patients treated by long-term dialysis compared with the general population. Am J Kidney Dis. 2012;59:819–28.
8. Webster AC, Nagler EV, Morton RL, Masson P. Chronic kidney disease. Lancet. 2017;389:1238–52.
9. Breyer MD, Susztak K. The next generation of therapeutics for chronic kidney disease. Nat Rev Drug Discov. 2016;15:568–88.
10. Chen DQ, Feng YL, Cao G, Zhao YY. Natural products as a source for antifibrosis therapy. Trends Pharmacol Sci. 2018;39:937–52.
11. Hsu CL, Yen GC. Ganoderic acid and lucidenic acid (Triterpenoid). Enzymes. 2014;36:33–56.
12. Gill BS, Navgeet, Kumar S. Ganoderma lucidum targeting lung cancer signaling: a review. Tumor Biol 2017;39:1010428317707437. https://doi.org/10.1177/1010428317707437.
13. Zhong D, Wang H, Liu M, Li X, Huang M, Zhou H, et al. Ganoderma lucidum polysaccharide peptide prevents renal ischemia reperfusion injury via counteracting oxidative stress. Sci Rep 2015;5:16910.
14. He J, Sun Y, Jia Y, Geng X, Chen R, Zhou H, et al. Ganoderma triterpenes protect against hyperhomocysteinemia induced endothelial-mesenchymal transition via TGF-beta signaling inhibition. Front Physiol. 2019;10:192.
15. Su L, Liu L, Jia Y, Lei L, Liu J, Zhu S, et al. Ganoderma triterpenes retard renal cyst development by downregulating Ras/MAPK signaling and promoting cell differentiation. Kidney Int. 2017;92:1404–18.

16. Zhong D, Xie Z, Huang B, Zhu S, Wang G, Zhou H, et al. Ganoderma lucidum polysaccharide peptide alleviates hepatoteatosis via modulating bile acid metabolism dependent on FXR-SHP/FGF. Cell Physiol Biochem. 2018;49:1163–79.
17. Lu J, Qin JZ, Chen P, Chen X, Zhang YZ, Zhao SJ. Quality difference study of six varieties of ganoderma lucidum with different origins. Front Pharmacol. 2012;3:57.
18. Jiang J, Grieb B, Thyagarajan A, Sliva D. Ganoderic acids suppress growth and invasive behavior of breast cancer cells by modulating AP-1 and NF-kappaB signaling. Int J Mol Med. 2008;21:577–84.
19. Zhang X, Xiao C, Liu H. Ganoderic acid A protects rat H9c2 cardiomyocytes from hypoxia-induced injury via up-regulating miR-182-5p. Cell Physiol Biochem. 2018;50:2086–96.
20. Cao FR, Feng L, Ye LH, Wang LS, Xiao BX, Tao X, et al. Ganoderic acid A metabolites and their metabolic kinetics. Front Pharmacol. 2017;8:101.
21. Lin DM, Wang SZ, Luo HJ, Lin ZX, Lin SQ. Rapid separation of ganoderic acid from the extraction by-products of *Ganoderma lucidum*. Fujian Med J. 2018;40:135–8.
22. Chevalier RL, Forbes MS, Thornhill BA. Ureteral obstruction as a model of renal interstitial fibrosis and obstructive nephropathy. Kidney Int. 2009;75:1145–52.
23. Bao YW, Yuan Y, Chen JH, Lin WQ. Kidney disease models: tools to identify mechanisms and potential therapeutic targets. Zool Res. 2018;39:72–86.
24. Jia Y, He J, Wang L, Su L, Lei L, Huang W, et al. Dapagliflozin aggravates renal injury via promoting gluconeogenesis in *db/db* mice. Cell Physiol Biochem. 2018;45:1747–58.
25. Wang W, Li F, Sun Y, Lei L, Zhou H, Lei T, et al. Aquaporin-1 retards renal cyst development in polycystic kidney disease by inhibition of Wnt signaling. FASEB J. 2015;29:1551–63.
26. Wang W, Geng X, Lei L, Jia Y, Li Y, Zhou H, et al. Aquaporin-3 deficiency slows cyst enlargement in experimental mouse models of autosomal dominant polycystic kidney disease. FASEB J. 2019. https://doi.org/10.1096/fj.201801338RRR.
27. Pillai TG, John M, Sara Thomas G. Prevention of cisplatin induced nephrotoxicity by terpenes isolated from *Ganoderma lucidum* occurring in southern parts of India. Exp Toxicol Pathol. 2011;63:157–60.
28. Lan HY. Smad7 as a therapeutic agent for chronic kidney diseases. Front Biosci. 2008;13:4984–92.
29. Watanabe H, de Caestecker MP, Yamada Y. Transcriptional cross-talk between Smad, ERK1/2, and p38 mitogen-activated protein kinase pathways regulates transforming growth factor-beta-induced aggrecan gene expression in chondrogenic ATDC5 cells. J Biol Chem. 2001;276:14466–73.
30. Hung TW, Tsai JP, Lin SH, Lee CH, Hsieh YH, Chang HR. Pentraxin 3 activates JNK signaling and regulates the epithelial-to-mesenchymal transition in renal fibrosis. Cell Physiol Biochem. 2016;40:1029–38.
31. Stambe C, Atkins RC, Tesch GH, Masaki T, Schreiner GF, Nikolic-Paterson DJ. The role of p38alpha mitogen-activated protein kinase activation in renal fibrosis. J Am Soc Nephrol. 2004;15:370–9.
32. Feng Y, Ren J, Gui Y, Wei W, Shu B, Lu Q, et al. Wnt/beta-catenin-promoted macrophage alternative activation contributes to kidney fibrosis. J Am Soc Nephrol. 2018;29:182–93.
33. Chen Z, Sun J, Li T, Liu Y, Gao S, Zhi X, et al. Iron chelator-induced up-regulation of Ndrg1 inhibits proliferation and EMT process by targeting Wnt/beta-catenin pathway in colon cancer cells. Biochem Biophys Res Commun. 2018;506:114–21.
34. Zhang J, Cai H, Sun L, Zhan P, Chen M, Zhang F, et al. LGR5, a novel functional glioma stem cell marker, promotes EMT by activating the Wnt/beta-catenin pathway and predicts poor survival of glioma patients. J Exp Clin Cancer Res. 2018;37:225.
35. Chi B, Wang S, Bi S, Qin W, Wu D, Luo Z, et al. Effects of ganoderic acid A on lipopolysaccharide-induced proinflammatory cytokine release from primary mouse microglia cultures. Exp Ther Med. 2018;15:847–53.
36. Chang Y, Kong R. Ganoderic acid A alleviates hypoxia-induced apoptosis, autophagy, and inflammation in rat neural stem cells through the PI3K/AKT/mTOR pathways. Phytother Res. 2019;33:1448–56.
37. Ai J, Nie J, He J, Guo Q, Li M, Lei Y, et al. GQ5 hinders renal fibrosis in obstructive nephropathy by selectively inhibiting TGF-beta-induced smad3 phosphorylation. J Am Soc Nephrol. 2015;26:1827–38.
38. Wang W, Huang XR, Li AG, Liu F, Li JH, Truong LD, et al. Signaling mechanism of TGF-beta1 in prevention of renal inflammation: role of Smad7. J Am Soc Nephrol. 2005;16:1371–83.
39. Liu Y. Epithelial to mesenchymal transition in renal fibrogenesis: pathologic significance, molecular mechanism, and therapeutic intervention. J Am Soc Nephrol. 2004;15:1–12.
40. Kalluri R, Neilson EG. Epithelial-mesenchymal transition and its implications for fibrosis. J Clin Investig. 2003;112:1776–84.
41. Rastaldi MP. Epithelial-mesenchymal transition and its implications for the development of renal tubulointerstitial fibrosis. J Nephrol. 2006;19:407–12.
42. Liu Y. New insights into epithelial-mesenchymal transition in kidney fibrosis. J Am Soc Nephrol. 2010;21:212–22.
43. Lovisa S, LeBleu VS, Tampe B, Sugimoto H, Vadnagara K, Carstens JL, et al. Epithelial-to-mesenchymal transition induces cell cycle arrest and parenchymal damage in renal fibrosis. Nat Med. 2015;21:998–1009.
44. Meng XM, Nikolic-Paterson DJ, Lan HY. TGF-beta: the master regulator of fibrosis. Nat Rev Nephrol. 2016;12:325–38.
45. Sato M, Muragaki Y, Saika S, Roberts AB, Ooshima A. Targeted disruption of TGF-beta1/Smad3 signaling protects against renal tubulointerstitial fibrosis induced by unilateral ureteral obstruction. J Clin Investig. 2003;112:1486–94.
46. Li Y, Shen Y, Li M, Su D, Xu W, Liang X, et al. Inhibitory effects of peroxisome proliferator-activated receptor gamma agonists on collagen IV production in podocytes. Mol Cell Biochem. 2015;405:233–41.
47. Rhyu DY, Yang Y, Ha H, Lee GT, Song JS, Uh ST, et al. Role of reactive oxygen species in TGF-beta1-induced mitogen-activated protein kinase activation and epithelial-mesenchymal transition in renal tubular epithelial cells. J Am Soc Nephrol. 2005;16:667–75.
48. Thornton TM, Pedraza-Alva G, Deng B, Wood CD, Aronshtam A, Clements JL, et al. Phosphorylation by p38 MAPK as an alternative pathway for GSK3 beta inactivation. Science. 2008;320:667–70.
49. Ellenrieder V, Hendler SF, Boeck W, Seufferlein T, Menke A, Ruhland C, et al. Transforming growth factor beta1 treatment leads to an epithelial-mesenchymal transdifferentiation of pancreatic cancer cells requiring extracellular signal-regulated kinase 2 activation. Cancer Res. 2001;61:4222–8.
50. Lv ZM, Wang Q, Wan Q, Lin JG, Hu MS, Liu YX, et al. The role of the p38 MAPK signaling pathway in high glucose-induced epithelial-mesenchymal transition of cultured human renal tubular epithelial cells. PLoS One. 2011;6:e22806.
51. Pat B, Yang T, Kong C, Watters D, Johnson DW, Gobe G. Activation of ERK in renal fibrosis after unilateral ureteral obstruction: modulation by antioxidants. Kidney Int. 2005;67:931–43.
52. Li Z, Liu X, Wang B, Nie Y, Wen J, Wang Q, et al. Pirfenidone suppresses MAPK signalling pathway to reverse epithelial-mesenchymal transition and renal fibrosis. Nephrology. 2017;22:589–97.
53. Pardali E, Sanchez-Duffhues G, Gomez-Puerto MC, Ten Dijke P. TGF-beta-induced endothelial-mesenchymal transition in fibrotic diseases. Int J Mol Sci. 2017;18:2157.
54. Syed V. TGF-beta signaling in cancer. J Cell Biochem. 2016;117:1279–87.
55. MacFarlane EG, Haupt J, Dietz HC, Shore EM. TGF-beta family signaling in connective tissue and skeletal diseases. CSH Perspect Biol. 2017;9:a022269.
56. Radwan FF, Hossain A, God JM, Leaphart N, Elvington M, Nagarkatti M, et al. Reduction of myeloid-derived suppressor cells and lymphoma growth by a natural triterpenoid. J Cell Biochem. 2015;116:102–14.
57. Das A, Miller R, Lee P, Holden CA, Lindhorst SM, Jaboin J, et al. A novel component from citrus, ginger, and mushroom family exhibits antitumor activity on human meningioma cells through suppressing the Wnt/beta-catenin signaling pathway. Tumor Biol. 2015;36:7027–34.